

A comparative study between diffraction analysis softwares and measured motions

Auteur : Ei Phyu Sin Mon,

Promoteur(s) : 14997

Faculté : Faculté des Sciences appliquées

Diplôme : Master : ingénieur civil mécanicien, à finalité spécialisée en "Advanced Ship Design"

Année académique : 2020-2021

URI/URL : <http://hdl.handle.net/2268.2/13266>

Avertissement à l'attention des usagers :

Tous les documents placés en accès ouvert sur le site le site MatheO sont protégés par le droit d'auteur. Conformément aux principes énoncés par la "Budapest Open Access Initiative"(BOAI, 2002), l'utilisateur du site peut lire, télécharger, copier, transmettre, imprimer, chercher ou faire un lien vers le texte intégral de ces documents, les disséquer pour les indexer, s'en servir de données pour un logiciel, ou s'en servir à toute autre fin légale (ou prévue par la réglementation relative au droit d'auteur). Toute utilisation du document à des fins commerciales est strictement interdite.

Par ailleurs, l'utilisateur s'engage à respecter les droits moraux de l'auteur, principalement le droit à l'intégrité de l'oeuvre et le droit de paternité et ce dans toute utilisation que l'utilisateur entreprend. Ainsi, à titre d'exemple, lorsqu'il reproduira un document par extrait ou dans son intégralité, l'utilisateur citera de manière complète les sources telles que mentionnées ci-dessus. Toute utilisation non explicitement autorisée ci-avant (telle que par exemple, la modification du document ou son résumé) nécessite l'autorisation préalable et expresse des auteurs ou de leurs ayants droit.



With the support of the
Erasmus+ Programme
of the European Union



A COMPARATIVE STUDY BETWEEN DIFFRACTION ANALYSIS SOFTWARES AND MEASURED MOTIONS

MASTER THESIS (PUBLIC VERSION)

Submitted on : September 6, 2021

By : Ei Phyu Sin MON

Student ID : 200525E

Address : 2 Rue Maurice Monnier 44400 Reze

e-mail : eiphyusinmon.mmu@gmail.com

Supervisors : Benjamin Baert, DEME Group

Florian Stempinski, DEME Group

Reviewers : David Le Touze, Ecole Centrale de Nantes

Guillaume Ducrozet, Ecole Centrale de Nantes



Contents

List of Figures	iii
List of Tables	iv
1 Introduction	1
1.1 Convention	2
1.1.1 Reference Coordinates of the System	2
1.1.2 Wave Angle Conventions	2
1.2 Floating Rigid Motions	3
2 Theoretical Framework	4
2.1 Potential Flow Theory	4
2.1.1 Hypothesis of Potential Flow Theory	4
2.1.2 Solving Boundary Value Problems	4
2.1.3 Solving the Equation of Motion	6
3 Radiation and Diffraction Analysis	9
3.1 Radiation Diffraction Analysis with ANSYS-AQWA	10
3.1.1 Analysis Stages in AQWA	10
3.1.2 Mesh Convergence Study	10
3.2 Radiation Diffraction Analysis with Open Source BEM Code NEMOH	12
3.2.1 Application of NEMOH Solver	12
3.2.2 Importing the Geometry	13
3.2.3 Running NEMOH	13
3.3 Radiation Diffraction Analysis with Orcawave	15
3.3.1 Running Orcawave	15
4 Implementation of Viscous Roll Damping	15
5 Comparison of Results Obtained from three Radiation-Diffraction Softwares	16
6 Discussion of the Results from Radiation-Diffraction Software Packages	16

*A COMPARATIVE STUDY BETWEEN DIFFRACTIONANALYSIS SOFTWARES AND
MEASURED MOTIONS*

7 Ship Motions in Waves	18
7.1 Wave Spectra	18
7.2 Two Dimensional Wave Spectra	18
7.2.1 Plotting of Measured Wave Spectra	19
7.3 Standard Wave Spectra Models	20
7.3.1 Sea State Parameters	21
7.3.2 The Pierson-Moskowitz and JONSWAP spectra	21
7.3.3 Directional Spreading Function	22
7.3.4 Sensitivity Analysis for choosing Peak Shape Parameter γ	22
7.3.5 Implementation of Correction Term α in JONSWAP Wave Spectra	23
7.3.6 Comparison of Significant Wave Height and Peak Period	25
7.4 Response Spectra	27
7.4.1 Measured Response Spectra	27
7.4.2 JONSWAP Response Spectra	27
7.4.3 Significant Motions	27
8 Conclusion	28
References	30

List of Figures

1	Reference coordinates of the system[2]	2
2	Wave direction conventions	3
3	Six degree of freedom [3]	3
4	Ship A diffracted panels in AQWA GS	12
5	Ship B diffracted panels in AQWA GS	12
6	Overview of NEMOH [10]	12
7	Mesh output from <code>Mesh.exe</code> used in NEMOH	14
8	Convention used in Radar	19
9	Sea state representation from onboard measurement	20
10	Significant wave height and spectral energy for different γ Values	23
11	Comparison of spectral energy between measured and JONSWAP wave spectra with respect to frequency	24
12	Comparison of spectral energy between measured and JONSWAP wave spectra with respect to angle	24
13	Sea state representation from JONSWAP model	25

List of Tables

1	Different sizes of meshes chosen for mesh convergence study	11
2	Relative error with respect to finest mesh	11
3	Summary of three different diffraction software packages (ratings for accuracy: good and fair, ratings for computational cost: high, medium, low) . .	17
4	Significant wave height and peak period for onboard Measurement and JONSWAP Wave Spectra	26

ABSTRACT

Investigation of vessels' behaviors in waves are quite significant for the preparation of offshore operations. It impacts the workability and the integrity of the components to be installed (e.g. wind turbine, topside or foundation) for the offshore installation vessels. It is necessary to do radiation-diffraction analysis during the ship design phase and throughout the life span of the ship.

In the first part of the thesis, radiation-diffraction analyses are performed for three different software packages which are ANSYS-AQWA, Orcawave and NEMOH. The first two software packages are commercial software; therefore, the aim is to investigate the prospect of utilising open source code NEMOH for demonstrating the hydrostatic and hydrodynamics databases in terms of modelling and computational effort. Moreover, the preparation of input vessel geometries and post processing for the calculation of response amplitude operators (RAO), which are not available in ready to use format in NEMOH solver, are presented and validated the results. Then RAO which is one of the two main parts in motion calculation from three diffraction softwares are compared for all six degree of freedoms, 98 wave frequencies, 25 wave directions. Diffraction calculations are carried out for two offshore installation vessels which are currently in service at DEME offshore.

The second part of the thesis is the calculation of motion spectra from the RAOs and wave energy spectra. Firstly, wave energy spectra are taken from onboard measurement and post-processed into two dimensional spectra for 28 sea states. Secondly, the engineering wave spectra model JONSWAP is implemented by using the sea state parameters calculated from the measured energy spectra and modified to achieve a compromise between the measured energy spectra. Then the response spectra are computed from both measured wave spectra and JONSWAP. Then the significant motions for all degree of freedom and sea states are calculated from the response spectra and compared to each other. The method presented in this thesis for characterising suitable wave spectra and follow-up significant motion calculation are beneficial for normal working condition.

1 Introduction

Climate change and environmental degradation are an existential threat to Europe and all over the world. EU strives to become the first climate-neutral continent by 2050 [1], as emphasised in the European Green Deal, and offshore renewable is therefore of key importance. Offshore renewable energy covers several energy sources and various technologies, which are at different stages of development. A sustainable energy source that plays a big role in this energy transition is offshore wind energy. Since the demand for renewable energy is rising continuously and onshore space is constrained, more wind parks are being built at ocean. That is why, offshore installation vessels play the important role in the construction and maintenance of wind parks in an offshore environment.

In this thesis, investigation of the vessel behaviour is performed from two offshore installation vessels. In engineering, vessel behaviour can be calculated by using radiation-diffraction software packages and standard wave spectra. In this thesis, diffraction-radiation calculations are carried out by using three diffraction-radiation software packages including open source software. Subsequently motion calculations for various sea states are performed and compared with measured data. The comparison of measured motion is affected by the accuracy of response amplitude operators calculated from diffraction software packages and sea state definitions.

This thesis is carried with the collaboration of DEME Group, Belgium. DEME is a global solutions provider in the offshore energy, dredging, environmental and infra marine industry.

1.1 Convention

1.1.1 Reference Coordinates of the System

There are three axes in any ship, called longitudinal (x), transverse (y) and vertical axes (z).

In diffraction software packages such as NEMOH and AQWA, it is convenient to use the center of gravity or on the waterline of the aft perpendicular of the body as a reference point.

With conventional modelling, X is along the length of the vessel positive to bow, Y along the beam positive to port, and Z in the direction of the cross product of X and Y positive upwards. This axis system moves with the vessel.[2]

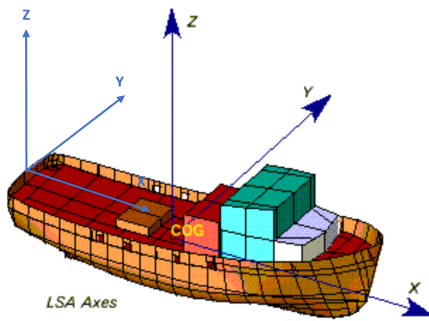


Figure 1: Reference coordinates of the system[2]

1.1.2 Wave Angle Conventions

The wave direction is defined as the angle from the positive global X axis to the direction in which the wave is travelling, measured anti-clockwise when seen from above. Therefore waves travelling along the X axis (from -X to +X) have a 0 degree wave direction, and waves travelling along the Y axis (from -Y to +Y) have a 90 degree wave direction. [2] On the flip side, the wave travelling along the X axis (from +X to -X) in the port side counts -180 to 0 degree in AQWA and 180 to 360 degree in NEMOH.

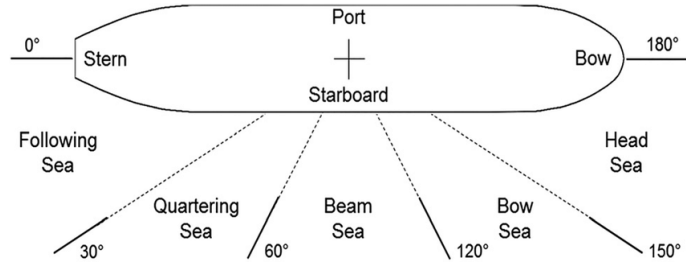


Figure 2: Wave direction conventions

1.2 Floating Rigid Motions

A ship operating in waves moves in all six degrees of freedom. Each axis has one translational and one rotational motion. These six DOFs are

- Surge is the linear motion in x-direction (longitudinal), positive forwards.
- Sway is the linear motion in y-direction (transversal), positive to port side.
- Heave is the linear motion in z-direction (vertical), positive upwards.
- Roll is the rotational motion around x-axis. Positive roll is when the port side is down and the starboard is up.
- Pitch is the rotational motion around y-axis. Pitch is positive when the bow is down relative to ship level.
- Yaw is the rotational motion around z-axis. When the bow moves in the port direction, we considered that a positive yaw angle.

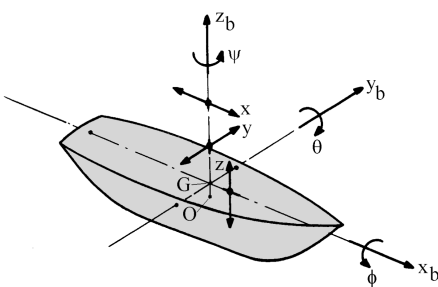


Figure 3: Six degree of freedom [3]

2 Theoretical Framework

This section covers the main components of the theories and assumptions for the calculations for the following chapters. The summary of linear potential flow theory, its hypothesis, solving the boundary value problems to obtain diffraction-radiation potentials are discussed. Eventually, solving the equation of motion from velocity potentials in order to get the response amplitude operators are presented.

2.1 Potential Flow Theory

2.1.1 Hypothesis of Potential Flow Theory

In seakeeping calculation, potential flow theory is used to calculate hydrodynamic coefficients (added masses, damping coefficients, wave forces) usually with Boundary Elements Methods with the assumption of large body (incoming wave is relatively small compared to the structure, $K_c \ll O(1)$ and K_c can be formulated as follows).

$$\text{Keulegan Carpenter Number: } KC = \frac{2\pi A}{L} \quad (1)$$

where A is the amplitude of the wave and L is the characteristic length of the structure.

In order to build this wave-structure interaction model, the necessary hypotheses concern both the fluid model and the boundary conditions.

Linear potential flow theory assumes that

- the fluid is isovolume without viscous effects which is considered as perfect fluid leading to Euler Model [4]. Perfect fluid is described as
 - inviscid (dynamic viscosity $\mu = 0$)
 - incompressible ($\operatorname{div} \vec{v} = 0$)
- And also the flow is considered as irrotational ($\vec{\omega} = \vec{0}$)

BEM makes use of velocity potential ϕ from which velocity field can be derived. This is expressed mathematically as $\vec{v} = \vec{\operatorname{grad}}\phi$.[5][4]

2.1.2 Solving Boundary Value Problems

To determine the velocity potential, boundary value problems have to be solved. The potential flow of undisturbed incident wave is $\phi(x, y, z, t)$. The equation of total potential

*A COMPARATIVE STUDY BETWEEN DIFFRACTIONANALYSIS SOFTWARES AND
MEASURED MOTIONS*

is given by:

$$\phi = \phi_i + \phi_p \quad (2)$$

where ϕ_i = Potential of undisturbed incident wave and ϕ_p =Potential of wave propagating from structure towards infinity. ϕ_p is further decomposed into two elementary potentials i.e. diffraction and radiation. The radiation potential has six degrees of freedom.

$$\phi_R = \sum_{i=1}^6 V_i \phi_{Ri} \quad (3)$$

Hence, the potential of wave propagating from the structure has seven components which are given as:

$$\phi_p = \phi_D + \sum_{i=1}^6 V_i \phi_{Ri} \quad (4)$$

The following paragraphs are the six boundary values problems needed to be solved for the diffraction and radiation velocity potentials. The first four are the same for radiation and diffraction but the last two are different in formulation.

- i The first one is solving the Laplace equation and this condition is applied inside fluid domains.

$$\Delta \phi_{D,Ri} = 0 \quad (5)$$

- ii The second one is kinematic free surface boundary condition. The free surface F is a streamline and there is no velocity flux through the surface. So, the normal velocity of a particle is equal to the normal velocity of the interface.

$$\nabla \phi_{D,Ri} + \nabla F + F_t = 0 \quad (6)$$

- iii The third condition is the dynamics free surface condition. It also applied at the free surface and it assures that there is an equilibrium of forces at the free surface i.e. $z=0$.

$$\frac{\partial \phi_{D,Ri}}{\partial t} + gz + \frac{1}{2} \nabla \phi_{D,Ri}^2 = 0 \quad (7)$$

- iv The fourth boundary value problem is the slip condition and applied at the sea bottom($z=-h$).

$$\frac{\partial \phi_{D,Ri}}{\partial n} = 0 \quad (8)$$

- v The fifth boundary value problem is body conditions which is applied on the body of the structure.

$$\begin{aligned}\frac{\partial \phi_D}{\partial n} &= -\frac{\partial \phi_I}{\partial n} \\ \frac{\partial \phi_{Ri}}{\partial n} &= n_i\end{aligned}\quad (9)$$

- vi The last one is the radiation condition for the waves propagating away from the body. The potential ϕ_p converges to zero with the increment of the distance from the body.

2.1.3 Solving the Equation of Motion

In this section, forces are calculated in order to solve the equation of motion.

$$[M]\ddot{X} = F_{WS} + F_{gravity} + F_{moorings} + F_{others} (\text{ wire , viscous ...}) \quad (10)$$

where F_{WS} = wave structure interaction force, $F_{gravity}$ = gravity forces, $F_{mooring}$ =mooring force.[6] Mass term can be defined as below,

$$M = \begin{bmatrix} M & 0 & 0 & 0 & 0 & 0 \\ 0 & M & 0 & 0 & 0 & 0 \\ 0 & 0 & M & 0 & 0 & 0 \\ 0 & 0 & 0 & I_{44} & I_{45} & I_{46} \\ 0 & 0 & 0 & I_{45} & I_{55} & I_{44} \\ 0 & 0 & 0 & I_{46} & I_{56} & I_{66} \end{bmatrix} \quad (11)$$

where M is the mass of the structure and I_{ii} are the inertia of the structure.

Wave structure interaction force is the combination of hydrostatic force, excitation force, radiation forces and drag forces. Effects of drag forces effects is considerably small for small Keulegan Carpenter number with large body assumption for the structures except at the resonance.

Hydrostatic force F_H is the difference between buoyancy and gravity force and can be formulated as $F_H = -K_H X$ where K_H is hydrostatic stiffness matrix and x is the dis-

placement.

$$K_H = \begin{bmatrix} 0 & 0 & 0 & 0 & 0 & 0 \\ 0 & 0 & 0 & 0 & 0 & 0 \\ 0 & 0 & K_{33} & K_{34} & K_{35} & 0 \\ 0 & 0 & K_{34} & K_{44} & K_{45} & 0 \\ 0 & 0 & K_{35} & K_{45} & K_{55} & 0 \\ 0 & 0 & 0 & 0 & 0 & 0 \end{bmatrix} \quad (12)$$

The hydrostatic coefficients in the stiffness matrix in equation-12 are mentioned in the equation-13 below.

$$\begin{aligned} K_{33} &= \rho g A_W \\ K_{34} &= \rho g \int_{A_W} y dS \\ K_{35} &= -\rho g \int_{A_W} x dS \\ K_{44} &= \rho g \int_{A_W} y^2 dS + \rho g V (z_c - z_G) = \rho g V \overrightarrow{GM}_\alpha \\ K_{45} &= -\rho g \int_{A_W} xy dS \\ K_{55} &= \rho g \int_{A_W} x^2 dS + \rho g V (z_c - z_G) = \rho g V \overrightarrow{GM}_\beta \end{aligned} \quad (13)$$

where A_w = wetted surface area, z_c = the center of buoyancy, z_G = the center of gravity and V =the volume of the structure.

Excitation forces and radiation force are the inertial forces arising from potential flow theory $\phi = \phi_I + \phi_D + \phi_R$, Pressure $p = -\rho \left(\frac{\partial \phi_I}{\partial t} + \frac{\partial \phi_D}{\partial t} + \frac{\partial \phi_R}{\partial t} + gy + \dots \right)$. The relationship between velocity potential ϕ and generalised body velocity ($V = \frac{d(X)}{dt}$) is

$$\frac{\partial \phi}{\partial n} = \sum_{i=1}^6 V_i n_i \Big|_{Sc} \quad (14)$$

where $i=1,..,6$ represents six degree of freedom. Excitation force is the combination of Froude-Krylov force and diffraction force. The Froude–Krylov force F_{FK} is the force introduced by the unsteady pressure field generated by undisturbed waves. [7]

$$\vec{F}_{FK} = \iint_{S_B} p_I \vec{n} ds = i\rho\omega \int_{Sco} \phi_i n_i ds \quad (15)$$

*A COMPARATIVE STUDY BETWEEN DIFFRACTIONANALYSIS SOFTWARES AND
MEASURED MOTIONS*

where \vec{F}_{FK} = Froude Krylov force, S_B =the wetted surface of the floating body, p_I is the pressure in the undisturbed waves and \vec{n} is the body's normal vector.

The Froude–Krylov force together with the diffraction force, make up the total non-viscous forces acting on a floating body in regular waves. The body interacts with the incident waves and it creates a diffracted wave on the free surface. There exists an unsteady pressure field p_D associated with the diffracted wave field. It can be formulated as

$$\vec{F}_D = \iint_{S_B} p_D \vec{n} dS = i\rho\omega \int_{Sco} \phi_D n_i ds \quad (16)$$

The unsteady motion of the body creates radiated waves. Hence the unsteady pressure fields created by radiated waves and the radiation force can be formulated as below

$$\vec{F}_R = \iint_{S_B} p_R \vec{n} dS = \sum_{j=1}^6 f_{ij} V_j \quad (17)$$

where f_{ij} =the radiation loads matrix and the load exerted in direction i , due to a unit velocity motion in the j degree of freedom. The total radiation load can be further detailed as below

$$\mathbb{R}_e (V_j f_{ji} e^{-i\omega t}) = - \left(\rho \int_{Sco} \mathbb{R}_e \phi_{Rj} n_i dS \right) \ddot{X}_j - \left(\rho \omega \int_{Sco} \mathbb{I}_m \phi_{Rj} n_i dS \right) \dot{X}_j \quad (18)$$

Radiation forces are composed of a term proportional to the body acceleration, and another one proportional to the body velocity. The first term behaves like added mass term ' A ' and the second one is damping term ' B '.

$$F_{Ri}(t) = - \sum_{j=1}^6 A_{ij} \ddot{X}_j(t) - \sum_{j=1}^6 B_{ij} \dot{X}_j(t) \quad (19)$$

Eventually, equation-10 becomes

$$[M]\ddot{X} = -K_H X + F_{excitation} + F_R + F_{drag} + F_{gravity} + F_{moorings} + F_{others} (\text{ wire , viscous ...}) \quad (20)$$

The hydrostatic and hydrodynamic (excitation and radiation) forces are only considered for the equation of motion and the other terms are neglected in equation 20. If we assume the wave input is unidirectional and monochromatic wave (regular wave with

single frequency), the response can be considered as harmonic $X(t)=\mathbb{R}_e(Xe^{-i\omega t})$ which is proportional to the incoming wave with amplitude $a(t)=ae^{-i\omega t}$. The matrix equation for the body motion becomes

$$([M] + [A])\ddot{X}(t) + [B]\dot{X}(t) + [K_H]X(t) = \mathbb{R}e[(F_I + F_D)e^{-i\omega t}] \quad (21)$$

Then

$$\{-\omega^2([M] + [A(\omega)]) + [K_H]\} - i\omega[B(\omega)] X = F_I + F_D = F_E \quad (22)$$

The terms in the equation-22 can be explained as follows, $[M]$ and $[K_H]$ depend on body characteristics (geometry and mass distribution).

$[A]$ and $[B]$ obtained by solving the 6 elementary radiation problems.

F_I depends on body geometry and incident wave.

F_D obtained by solving the diffraction problem in equation-16.

Then, if the amplitude of the incoming wave can be assumed as one unit, the component response amplitude operator 'RAO' can be calculated as

$$RAO = \frac{X}{a} = \frac{F_E}{\{-\omega^2([M] + [A(\omega)]) + [K_H] - i\omega[B(\omega)]\}} \quad (23)$$

RAOs are amplitude operators which enables to determine amplitude of motion based on a unitary wave which means that they are used to determine the likely behavior of a ship when operating at sea. RAOs are usually calculated for all wave headings and frequencies and for all ship motions.

3 Radiation and Diffraction Analysis

Radiation-Diffraction analysis is carried out for two different offshore installation vessels and three diffraction-radiation software packages have been utilized and compared with each other in this thesis.

All the calculation are performed for 98 wave frequencies in the range of 0.2 to 2 [rad/s] which the structure is most likely to encounter during its life span. Wave directions are in the range of -180 to 180 [deg] with 25 intervals. Water depth d as 100 [m] and density ρ 1025 [kg/m³] are considered for all calculation.

3.1 Radiation Diffraction Analysis with ANSYS-AQWA

For this diffraction calculation, ANSYS-AQWA 18.1 package is utilised. The 3D model is being modelled by ANSYS design modeler or other 3D CAD software packages. Meshes are generated in AQWA GS 18.1 after importing .lin file (offset data) for ship A and in workbench for ship B.

3.1.1 Analysis Stages in AQWA

There are three analysis stages needed to carry out for the calculation of hydrodynamics database using AQWA suite.[8] They are:

- Stage 1- Input of Geometric Definition and Static Environment

Node and coordinate information of the vessels, material properties, geometric properties (inertia), water depth, water density and acceleration due to gravity are imported in this section. Hydrostatic properties such as center of gravity and inertia are calculated in this section. Thus, mass and hydrostatics stiffness matrices are obtained by running stage 1. These hydrostatic parameters are normally considered to remain constant for an analysis of a particular structure.

- Stage 2- Input of the Radiation/Diffraction Analysis Parameters

The information input in these data categories relate to the equation of motion of a diffracting structure in regular waves, for the specified wave frequencies and directions ranges. The data input are wave frequencies, directions and hydrostatic database calculated from stage 1.

- Stage 3- The Radiation/Diffraction Analysis

From the input parameter and result of Stage 1 and 2, added mass, damping, critical damping percentage, diffraction forces, Froude Krylov Forces,displacement RAO, velocity RAO and acceleration RAO and wave drift loads are calculated in this stage.

3.1.2 Mesh Convergence Study

Before calculation of hydrodynamic database, the underwater part of the hull needs to be discretized as surface mesh. In order to determine our optimal mesh and the idea is to find a compromise between the CPU time and the accuracy, mesh convergence study

*A COMPARATIVE STUDY BETWEEN DIFFRACTIONANALYSIS SOFTWARES AND
MEASURED MOTIONS*

is performed. The geometry of the ship A is given as offsets table and different sizes of mesh are created in AQWA GS 18.1. Only half of the hull is imported and the chosen six mesh sizes for mesh convergence study are described as follows

Mesh Size[m]	0.5	1	1.5	2	2.5	3
No. of elements [-]	55442	14481	6695	3773	2523	1835
No. of diffracting elements [-]	13393	3393	1562	868	569	411
Computation Time [s]	169612	15206	7603	831	310	149

Table 1: Different sizes of meshes chosen for mesh convergence study

Theoretically, the finest mesh gives the most accurate result but computation cost is significantly high. So, the relative errors with the finest mesh considered 0.5 m for different mesh sizes are analysed.

For this purpose, significant motions calculated from chosen mesh sizes by utilising AQWA FER are chosen as measure of convergence. These simulations are done for all 98 wave frequencies, 13 wave directions and 6 degree of freedom for RAO calculation and JONSWAP wave spectrum with $\gamma=3.3$, T_p between 4 to 10 [s] and $H_s=2\text{m}$ is used for input wave. Significant motion results are taken as the measure in convergence test. As a remark, the significant motion calculation from AQWA FER is performed only for this section and more detailed calculation about the significant motion will be explained in section-7.4. The error percentage with respect to the finest mesh in significant motions for six degrees of freedom are plotted as follows,

Element Size [m]	0.5	1	1.5	2	2.5	3
Relative Error with respect to finest mesh (%)						
Surge	0	-0.13	-0.05	-0.48	-1.57	-18.07
Sway	0	-0.58	-0.60	-0.93	-2.89	-40.95
Heave	0	-1.26	-1.14	-0.83	-0.90	-33.60
Roll	0	-0.79	9.52	8.07	-11.95	-18.63
Pitch	0	-0.01	0.00	0.06	-2.00	-2.00
Yaw	0	0.01	-0.29	-0.43	-8.03	-8.03

Table 2: Relative error with respect to finest mesh

As it can be seen in the above table, 2m mesh with 868 elements has relative error percentage less than 1% with respect to finest mesh except for roll DOF. Moreover the computation time is also quite less compared to finer meshes. So, the optimal mesh size is chosen as 2 m for ship A and used for further calculation. The figures below are hidden because of confidential information.

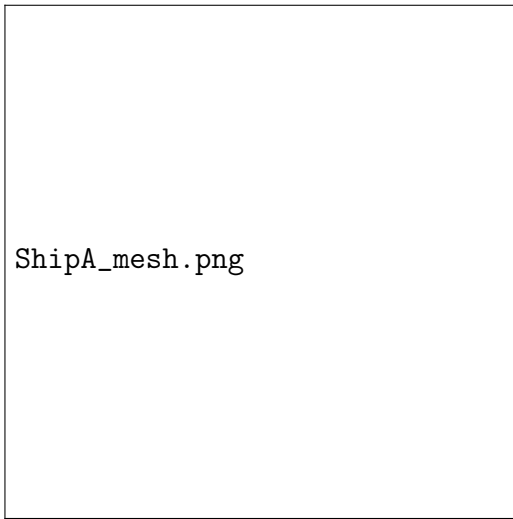


Figure 4: Ship A diffracted panels in AQWA GS

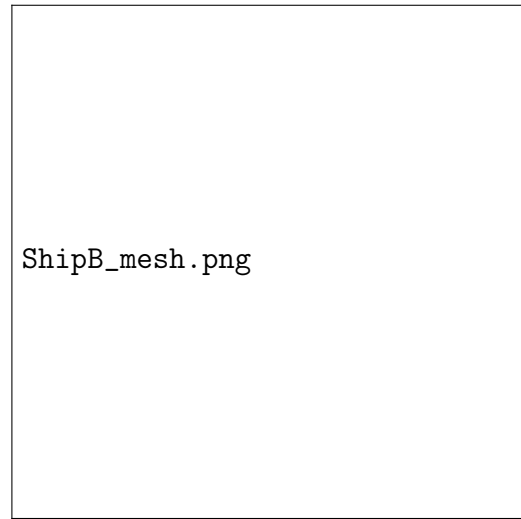


Figure 5: Ship B diffracted panels in AQWA GS

3.2 Radiation Diffraction Analysis with Open Source BEM Code NEMOH

3.2.1 Application of NEMOH Solver

NEMOH is an open source code of Boundary Element Methods (BEM) which dedicated to the computation of first order wave loads on offshore structures created in Ecole Central Nantes released publicly in 2014.[9] It can calculate added mass, radiation damping and excitation force. The hydrodynamic database is computed using linear potential flow theory and opposed to AQWA the response of the structure in 6 DOFs need to be post-processed in frequency domain by solving the equation of motion.

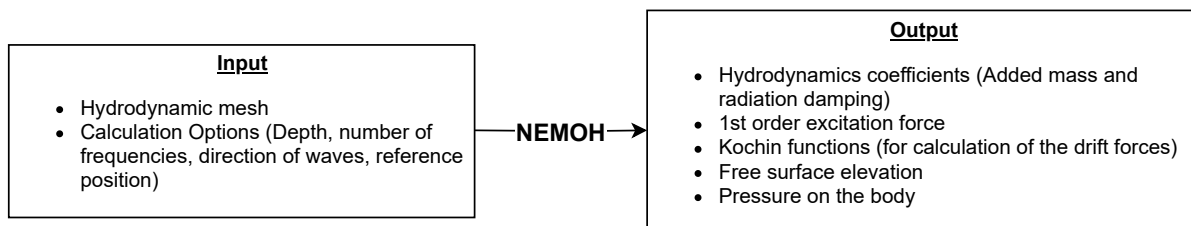


Figure 6: Overview of NEMOH [10]

Kochin functions, free surface elevation and pressure on the body are not be discussed in this thesis. Python package Capytain making use of NEMOH solver which is further not considered in this thesis.

3.2.2 Importing the Geometry

The mesh file created from ANSYS AQWA in the .dat file has to be converted to NEMOH. AQWA mesh file has both quadrilateral and triangular panels but NEMOH can handle only quadrilateral mesh. An operation needs to convert triangular meshes into quadrilateral meshes. For this purpose, the last nodes of all triangular meshes are duplicated to create the quadrilateral panels. A matlab script needs to be prepared for this operation. By doing this, quadrilateral panels can be obtained without changing the original shape of triangular meshes. [11]

Another important thing to note is that the phase of the incident wave is aligned with reference point (0,0,0) in NEMOH and that point should be the center of gravity location. In AQWA, the phase is aligned with center of gravity but the reference co-ordinate (0,0,0) is at the aft of the ship, on the waterline and on the centerline of the structure. So, another operation is necessary to carry out to shift the reference point of the AQWA into the center of gravity on X axis. All nodes defined in the input mesh .dat file are shifted towards the COG.

3.2.3 Running NEMOH

Before running NEMOH, the user has to make sure the following input files are present in the working directory. [12]

1. Mesh file- It is the mesh file of the geometry created by another meshing tools such as workbench .dat or rhinoceros .gdf format. If there is no readily available mesh file in these formats, one can generate mesh from axiMesh.m for axisymmetric mesh or mesh.m non axisymmetric meshes with MATLAB.
2. ID.dat- This file is used for identifying the calculation. It must be located in the working folder where the codes are run.
3. input.txt-This file is used for selecting the solver type. Currently, there are two options available, direct gauess or iterative GMRES (Generalized minimal residual method) solver.

4. Nemoh.cal- It is the most important input file because it provides the input of the calculation parameters such as environment (density, water depth,...), number of bodies (single or double body), name of the mesh file, number of wave frequencies and directions and number of DOFs, etc. nemoh.cal files are attached in the appendix I .

Then mesh.exe is also necessary to be present in the working folder which is the compiled mesher executable. The mesher takes this geometry as an input, and may divide some panels to try to match the targeted number of panels. The following figure is hidden because of confidential information.

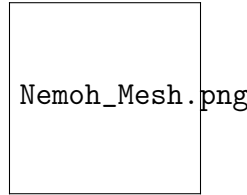


Figure 7: Mesh output from `Mesh.exe` used in NEMOH

The geometry of the ships is imported only half to run the NEMOH, full body in figure-7 is only for visualisation purposes.

After importing the above files, the following three `.exe` in NEMOH can be run step by step. They are

- **preprocessor.exe**

The aim of the preprocessor is to prepare the mesh and to generate the body conditions for each calculation case (radiation and diffraction) which are defined in the input file Nemoh.cal. Froude Krylov forces, body conditions for the calculation cases are generated from preprocessor.

- **solver.exe**

The aim of the solver is to solve the linear boundary value problems for each problem defined in the result file from postprocessor. The calculation depends on parameters which are read in the file input.txt (solver type) located in the working folder.

- **postprocessor.exe**

The aim of the postprocessor is to postprocess the results in order to provide the

relevant quantities (added mass, radiation damping, excitation force) in the usual format. It also provides a framework to make relevant calculations.

After obtaining the hydrostatic and hydrodynamics database from NEMOH, the equation of motion is implemented in MATLAB to perform post processing of the results from NEMOH so as to generate response amplitude operators RAO as shown in equation-23.

The results of hydrostatic and hydrodynamic database and RAO are discussed in section-??.

3.3 Radiation Diffraction Analysis with Orcawave

OrcaWave 11.b is a diffraction analysis program which calculates loading and response for wet bodies due to surface water waves via potential flow theory.[13]

The mesh files of the ships are imported into orcabwave with the format of .dat from AQWA.

3.3.1 Running Orcawave

In Orcawave, various mesh file from different meshing tools can be imported such as wamit gdf, AQWA dat, NEMOH dat, etc. OrcaWave has two linear solvers i) Direct LU ii) Iterative AGS. Potential formulation is the type of diffraction problem that is used. Center of gravity locations, mass of the ships and inertia matrix with respect to body origin are imported before running the simulation. After that, the following output are obtained from Orcawave.

- Hydrostatic stiffness matrix
- Added mass and damping matrices
- Load RAOs (Excitation Forces)
- Displacement RAOs

4 Implementation of Viscous Roll Damping

This section is not presented here because of confidential information of the company.

5 Comparison of Results Obtained from three Radiation-Diffraction Softwares

This section isn't displayed here since the results are obtained by private data of the company.

6 Discussion of the Results from Radiation-Diffraction Software Packages

First of all, hydrodynamic coefficients such as added mass, radiation damping and excitation forces are quite the same from all software packages. In RAO calculations, the results obtained from Orcawave is slightly different from AQWA. So, it can be concluded that all software packages give the results with good accuracy.

Although accuracy of the results plays the major role in engineering calculations, the other factors such as user-friendliness, computation time, price and documentation of the softwares are also important to consider. Since AQWA and Orcawave are commercial softwares, they have efficient computational capacity. On the other hand, the computation time in NEMOH is significantly higher compared to other two softwares. Details of computational hours cannot be described because different device is utilised in NEMOH simulation. The availability of multithreading in AQWA and OrcaWave also well explain the good efficiency in computation cost.

AQWA is the matured software; thus, it has a lot of reference documentation and validations with experimental results. Furthermore, AQWA is frequently used software in industrial applications as a radiation and diffraction analysis tool in order to determine the wave loads and RAOs. Therefore, the accuracy of NEMOH and Orcawave results are described by putting them in comparison with the AQWA results; considering the AQWA results as the most accurate. Although Orcawave is a new commercial software, its documentation is well defined and there are validation cases for Orcawave by comparing with other linear potential wave theory based softwares such as AQWA and WAMIT; however, no validation case established with NEMOH as yet.

In NEMOH, it's restricted to calculations in waves for structures with zero Froude numbers i.e. zero forward speed. The summary of the comparison of three different radiation-diffraction softwares are presented in the table below.

*A COMPARATIVE STUDY BETWEEN DIFFRACTIONANALYSIS SOFTWARES AND
MEASURED MOTIONS*

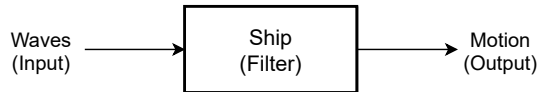
	AQWA	NEMOH	ORCAWAVE
Accuracy of Result	-	Good	Fair
Price	Commercial	Free	Commercial
Documentation and Validation	Good	Poor	Fair
User Friendliness	Medium	Poor	Good
QTF matrix calculation	YES	NO	YES
Adding Forward Speed	YES	NO	NO
Multithreading	YES	NO	YES
Computation Cost	Medium	High	Low
Calculation of Irregular Frequencies	YES	NO	YES

Table 3: Summary of three different diffraction software packages (ratings for accuracy: good and fair, ratings for computational cost: high, medium, low)

The results of RAO in all wave directions are described in Appendix.

7 Ship Motions in Waves

The ship could be treated as the black box in electrical filter which receives the waves as an input and generates motions as output. The output ship motion is directly proportional to the input waves as long as the filter is considered as linear. [14]



7.1 Wave Spectra

The first task to apply the electronic filter analogy is that the ship experiences the wave spectrum. Short term stationary irregular sea states may be described by a wave spectrum; that is, the power spectral density function of the vertical sea surface displacement.[15] Energy spectral density describe how energy is distributed over frequencies. Energy spectral density is derived from variance of free surface elevation denoted as ' σ^2 '.

$$Var[\eta(t)] = \sigma^2 = \frac{1}{T} \int_0^T \eta^2(t) dt = \frac{1}{2} a^2 \quad (24)$$

where T is the duration of the wave, η is the wave elevation and a is the amplitude of the wave. So variance spectral energy $S(f)$ can be described as

$$S(f) = \frac{\frac{1}{2} a^2}{\Delta f} \quad (25)$$

where Δf is the frequency band width.

In reality, ocean waves cannot be portrayed by single wave spectrum with frequency only. Directional wave spectra with the consideration of different wave directions are more realistic.

7.2 Two Dimensional Wave Spectra

The two-dimensional spectrum describes how the mean sea-surface elevation variance due to ocean waves is distributed as a function of frequency and propagation direction. The variance spectrum is discretised over a number of frequencies and directions. Two dimensional wave spectra can be expressed by the formula mentioned below.

$$S(f, \theta) = S(f)D(\theta, f) = S(f)D(\theta) \quad (26)$$

where $S(f, \theta)$ is the directional wave spectral density function or directional wave spectrum and $D(\theta, f)$ is the wave frequency dependent directional spreading function or spreading function. θ is the angle between the direction of elementary wave trains and the main wave direction of the short crested wave system.

7.2.1 Plotting of Measured Wave Spectra

It is common to assume that the sea surface is stationary for a duration of 20 minutes to 3 to 6 hours. In this thesis, real time measurement of directional wave spectra for 28 sea states are processed to describe two dimensional wave spectra.

The detail information of radar is hidden in public version.

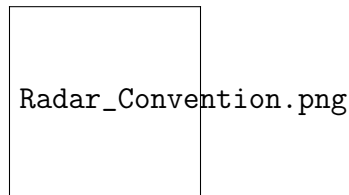


Figure 8: Convention used in Radar

Two dimensional frequency-direction spectrum with respect to spectral energy $S(f, \theta)$ as a function of frequency f and direction θ are given in ASCII format. This format contains calibrated spectral energy with the unit of $[m^2/(Hz \cdot rad)]$ and the spectral energy is in 2D matrix with the dimension of frequency and direction. The provided spectral data cannot be readily used for our purposes. That is why, processing and plotting of 2D spectrum data will be carried out through Python codes.

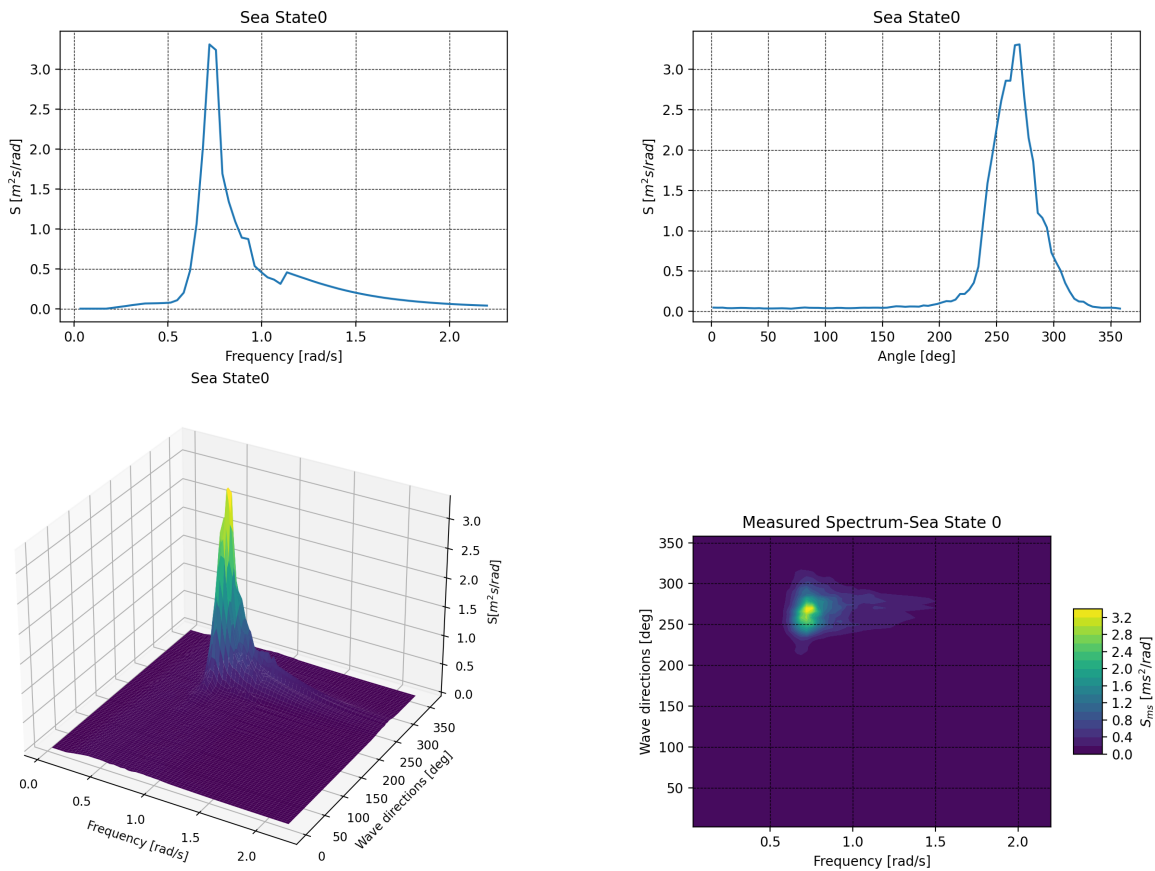


Figure 9: Sea state representation from onboard measurement

In figure 9, spectra energy is plotted with respect to frequency range $[0.0345 - 2.199]$ rad/s with 64 intervals and wave directions between $[2 - 378]$ deg with 90 intervals for the first sea state. The remaining sea states can be seen in appendix II.

7.3 Standard Wave Spectra Models

In most of the cases, real time measurement for various sea states cannot be readily accessible. So, it is necessary to apply standard wave spectra models in order to guess the real sea state. Models of the wave spectrum are widely used to simulate the sea surface in estimating prospects of new algorithms for radar data processing, schemes of measurement, and development of new radars. The following sea state parameters are needed to calculate from the real time measurement or assigned by the most suitable values if real time measurement is not available in order to create wave spectra. In this report, important parameters such as H_s and T_p will be calculated by the following formulations in section 7.3.1 from the real time measurement.

7.3.1 Sea State Parameters

In order to get significant wave height H_s and peak period T_p from the wave spectra, it is mandatory to figure it out spectral moments m_n . The following formulations are taken from DNV-GL guidelines. [15].

The spectral moments m_n of general order n are defined as

$$m_n = \int_0^{\infty} f^n S(f) df \quad (27)$$

where f is the wave frequency for $n=0,1,2,\dots,n$ and $S(f)$ is the spectral energy density described in 7.1. The following sea state parameters can be defined in terms of spectral moments defined above.

The significant wave height $H_s \simeq H_{m0}$ is given by

$$H_{m0} = 4\sqrt{m_0} \quad (28)$$

The zero-up crossing period $T_z = T_{m02}$ can be estimated by

$$T_{m02} = \sqrt{\frac{m_0}{m_2}} \quad (29)$$

After that we can create the wave spectra model such as JONSWAP, Pierson-Moskowitz models,etc....

7.3.2 The Pierson-Moskowitz and JONSWAP spectra

For fully developed sea, Pierson-Moskowitz Spectrum model is used. It is written in the form of

$$S_{PM}(\omega) = \frac{5}{16} \cdot H_S^2 \omega_p^4 \cdot \omega^{-5} \exp\left(-\frac{5}{4} \left(\frac{\omega}{\omega_p}\right)^{-4}\right) \quad (30)$$

where $\omega_p = \frac{2\pi}{T_p}$ is the angular spectral peak frequency. After analyzing data collected during the Joint North Sea Wave Observation Project JONSWAP, found that the wave spectrum is never fully developed. It continues to develop through non-linear, wave-wave interactions even for very long times and distances. Hence an extra and somewhat artificial factor was added to the Pierson-Moskowitz spectrum in order to improve the fit to their measurements. The JONSWAP spectrum is thus a Pierson-Moskowitz spectrum

multiplied by non-dimensional peak shape parameter' γ '.

$$S_J(\omega) = S_{PM}(\omega)\gamma^{\exp\left(0.5\left|\frac{\omega-\omega_p}{\sigma\omega_p}\right|^2\right)} \quad (31)$$

where $S_J(\omega)$ = Pierson-Moskowitz spectrum,

γ = non-dimensional peak shape parameter

σ =spectral width parameter with $\sigma= \sigma_a=0.07$ for $\omega \leq \omega_p$ and $\sigma= \sigma_b=0.09$ for $\omega > \omega_p$

After that, T_p can be calculated by using zero crossing period ' T_z ' by using the following formula,

$$\frac{T}{T_p} = 0.7303 + 0.04936\gamma - 0.006556\gamma^2 + 0.0003610\gamma^3 \quad (32)$$

7.3.3 Directional Spreading Function

After calculating the spectrum ' $S(\omega)$ ' from usual wave spectra, directional spreading function ' $D(\theta)$ ' is necessary to be taken into account in order to implement two dimensional wave spectra as described in equation-26.

$$D(\theta) = \frac{2^{2s-1}}{\pi} \frac{\Gamma^2(s+1)}{\Gamma(2s+1)} \cos^{2s} \left(\frac{\theta - \theta_m}{2} \right) \quad -\pi \leq \theta - \theta_m \leq \pi \quad (33)$$

where s=spreading parameter, Γ = Gamma function and θ_m = Mean angle [5]. In this thesis, s=10 is chosen according to ISO 19901-Annex 8 [16].

7.3.4 Sensitivity Analysis for choosing Peak Shape Parameter γ

Peak shape parameter γ plays the important role in implementing JONSWAP spectra. Sensitivity test is conducted in order to choose the most suitable γ for significant wave height obtained around 1.5 [m]. Detail of choosing γ is not presented here because of confidential reference.

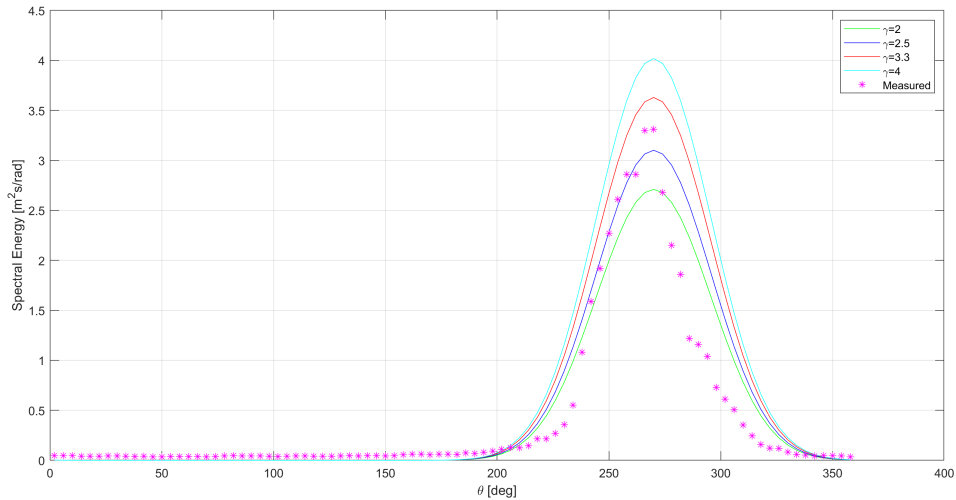


Figure 10: Significant wave height and spectral energy for different γ Values

According to figure-10, $\gamma = 3.3$ is chosen to proceed in generating of JONSWAP wave model. Correction term α in section- 7.3.5 is also utilised in the calculation energy spectra from JONSWAP in figure-10.

7.3.5 Implementation of Correction Term α in JONSWAP Wave Spectra

After creating the JONSWAP wave spectra from the formulation mentioned in section- 7.3.1, it can be noticed that the spectra energy obtained is much less compared to energy spectra from real time measurement and can be seen in figure-11. So, it is necessary to apply correction term in generating JONSWAP spectra. Here, correction term α is implemented according to significant wave height obtained from the measured spectra and JONSWAP spectra.

$$\alpha = \frac{H_{s_{radar}}}{H_{s_{JONSWAP}}} \quad (34)$$

where $H_{s_{radar}}$ is significant wave height calculated from measured spectral energy and $H_{s_{JONSWAP}}$ is significant wave height calculated from JONSWAP model. Thus, the formulation in equation-31 becomes

$$S_J(\omega) = \alpha^2 S_{PM}(\omega) \gamma^{\exp\left(0.5\left|\frac{\omega - \omega_p}{\sigma\omega_p}\right|^2\right)} \quad (35)$$

Figures-11,12 show the spectral energy with respect to wave frequencies and angles for real time measurement, JONSWAP and modified JONSWAP wave spectra.

*A COMPARATIVE STUDY BETWEEN DIFFRACTIONANALYSIS SOFTWARES AND
MEASURED MOTIONS*

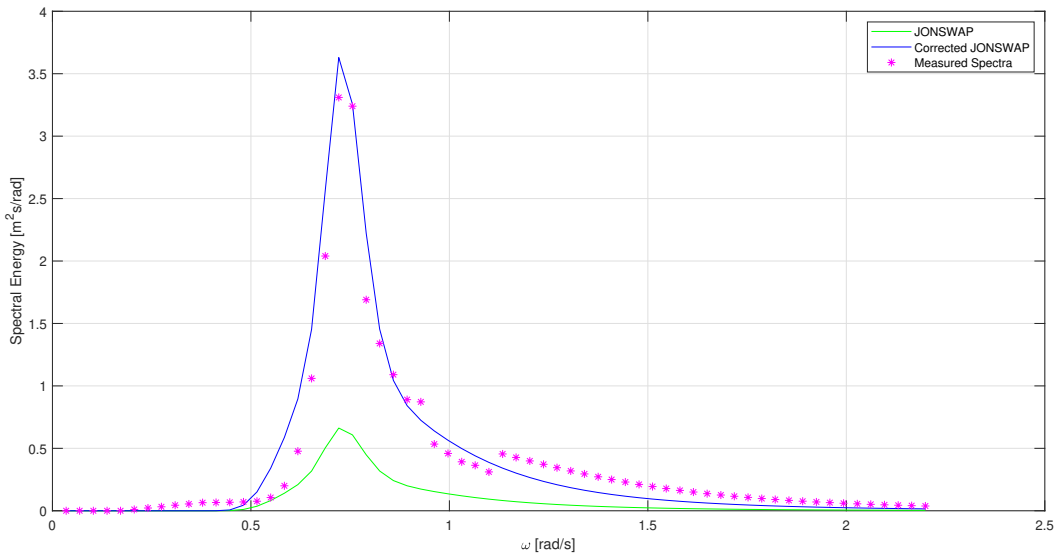


Figure 11: Comparison of spectral energy between measured and JONSWAP wave spectra with respect to frequency

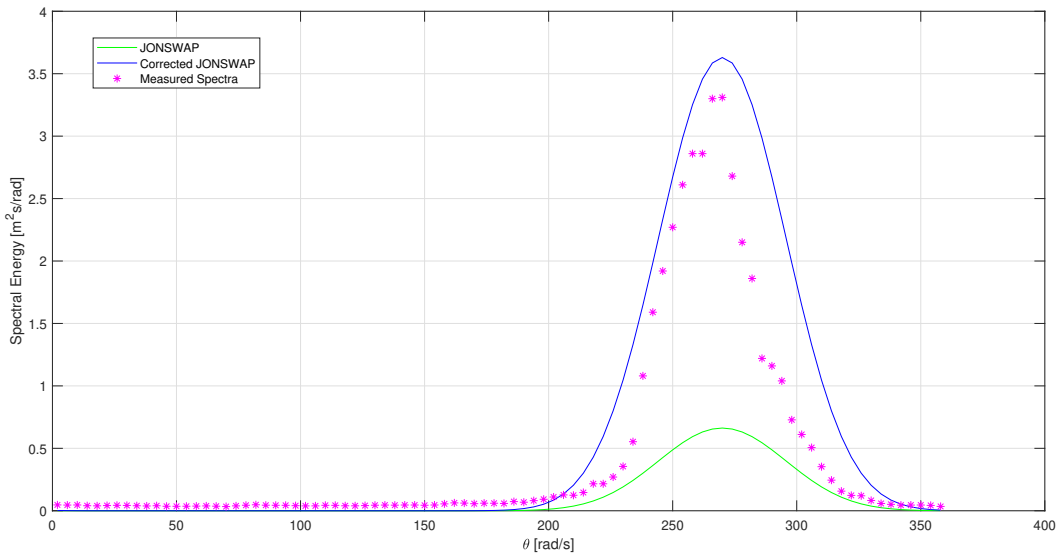


Figure 12: Comparison of spectral energy between measured and JONSWAP wave spectra with respect to angle

After applying sea state parameters (section 7.3.1), directional spreading function ' $D(\theta)$ ' (section 7.3.3), and JONSWAP formulation (equation-35), the most suitable wave spectra model is generated as shown in the figure-13. The following figures are plotted by using $H_s=1.55$ [m], $T_p=8.634$ [m] and $\gamma=2.5$ for the first sea state.

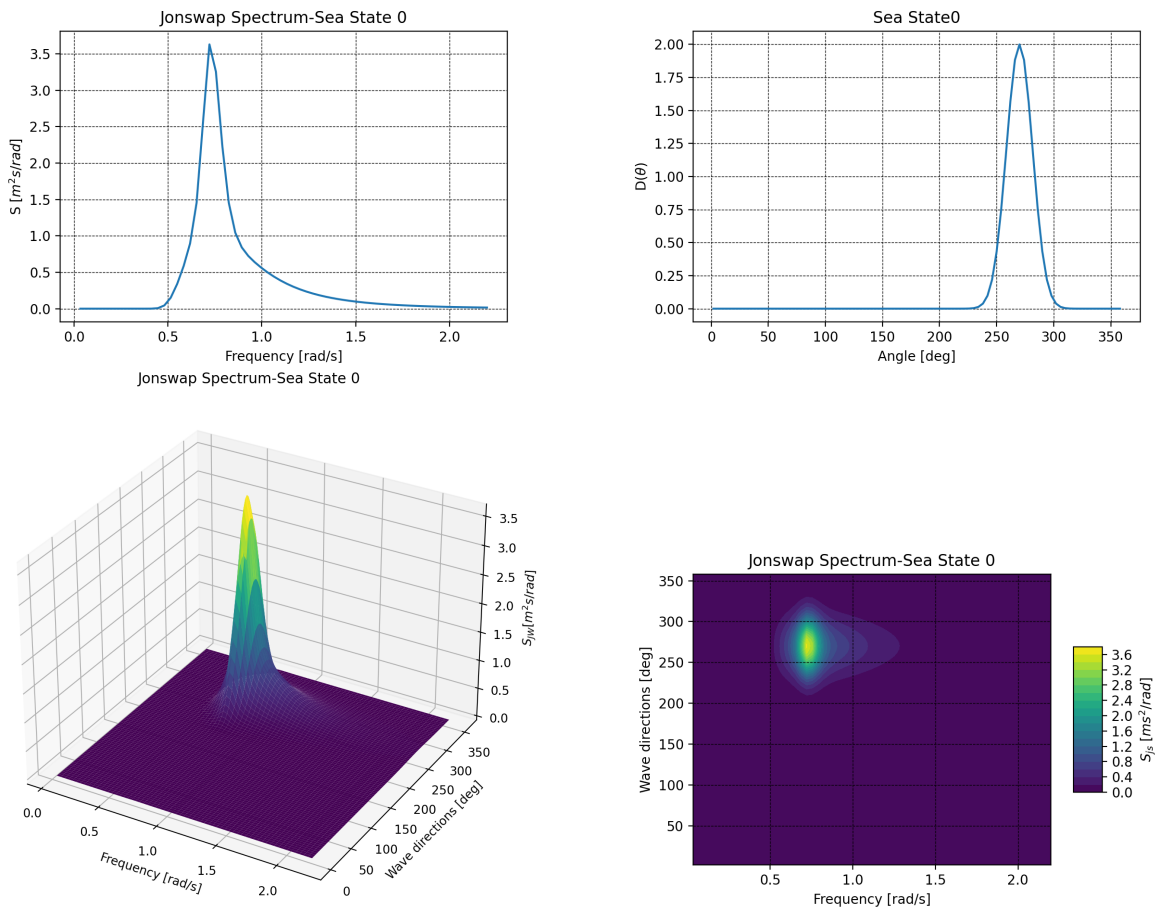


Figure 13: Sea state representation from JONSWAP model

The same intervals of frequencies and wave directions are taken as the measured energy spectra.

7.3.6 Comparison of Significant Wave Height and Peak Period

The following table shows the significant wave height and periods obtained from two wave models for all sea states.

	Wave Spectra			
	Real Time Measurement		JONSWAP	
Sea States	H_s [m]	T_p [s]	H_s [m]	T_p [s]
0	1.55	8.63	1.55	8.92
1	1.55	8.62	1.55	8.91
2	1.55	8.62	1.55	8.91
3	1.54	8.63	1.54	8.92
4	1.53	8.65	1.53	8.94

*A COMPARATIVE STUDY BETWEEN DIFFRACTIONANALYSIS SOFTWARES AND
MEASURED MOTIONS*

Table 4 continued from previous page

5	1.52	8.66	1.52	8.94
6	1.51	8.65	1.51	8.94
7	1.50	8.66	1.50	8.94
8	1.51	8.65	1.51	8.93
9	1.51	8.64	1.51	8.93
10	1.51	8.64	1.51	8.93
11	1.50	8.64	1.50	8.93
12	1.49	8.65	1.49	8.94
13	1.49	8.66	1.49	8.94
14	1.50	8.65	1.50	8.94
15	1.50	8.64	1.50	8.93
16	1.50	8.64	1.50	8.93
17	1.50	8.65	1.50	8.93
18	1.49	8.63	1.49	8.92
19	1.48	8.62	1.48	8.91
20	1.48	8.64	1.48	8.93
21	1.48	8.60	1.48	8.89
22	1.49	8.61	1.49	8.90
23	1.49	8.58	1.49	8.87
24	1.50	8.55	1.50	8.84
25	1.50	8.55	1.50	8.84
26	1.50	8.54	1.50	8.84
27	1.49	8.51	1.49	8.81

Table 4: Significant wave height and peak period for onboard Measurement and JONSWAP Wave Spectra

The significant wave heights of measured and Jonswap spectrum are exactly the same. As for the peak periods, the average discrepancy between these two is found to be 3.36%.

7.4 Response Spectra

As explained previously, the ships experience the waves and produces motions as output. In order to calculate the ship motions, we need to multiply wave energy spectra with ship transfer function values which is also referred to as Response Amplitude Operator with respect to wave frequencies and directions in all six degrees of freedom. Response amplitude operators 'RAO' are calculated from NEMOH for 98 wave directions, 64 frequencies and all degree of freedoms.

$$S_{res}(\omega, \theta) = S(\omega, \theta) |RAO^2| \quad (36)$$

where $S_{res}(\omega, \theta)$ = Response Energy Spectra, RAO= Response Amplitude Operator and $S(\omega, \theta)$ = Wave Spectral Energy.

7.4.1 Measured Response Spectra

In this section, response energy spectra for all degrees of freedom calculated from real time wave spectral energy are presented. The various response for the various degrees of freedom are obtained by using the relevant RAOs. The results of response spectra from onboard measurement are not shown in public version.

7.4.2 JONSWAP Response Spectra

Response spectral energy calculated by using JONSWAP wave spectra and corresponding response amplitude operators are presented in this section. The results of JONSWAP spectra from onboard measurement are not shown in public version.

7.4.3 Significant Motions

After calculating the response spectral energy from real time measurement and JONSWAP spectra $S_{res}(\omega, \theta)$ mentioned in sections-7.4.1 and 7.4.2, response or significant motions spectrum for all six degrees of freedom can also be calculated by the variance (0th order moment), m_{0res} of the 2D response spectrum

$$m_{0res}(\omega, \theta) = \int_0^{2\pi} \int_0^{\infty} S_{res}(\omega, \theta) d\omega d\theta \quad (37)$$

Then the response can be obtained by

$$\text{Response} = 2\sqrt{m_{0res}} \quad (38)$$

The results and observation of significant motions are not shown here because of confidentiality.

8 Conclusion

In the first part of the thesis, results of added mass, radiation damping and excitation forces from all diffraction software packages are well aligned through out the hydrodynamic analysis. Response amplitude operators post-processed from NEMOH are also matching very well with the direct output from ANSYS AQWA. Hence NEMOH can be considered as a good alternative for other commercial potential solvers despite having some weaknesses such as lack of calculating forward speed, suppressing irregular frequencies and parallel programming. But developers of NEMOH are trying to add these features so they will be available in the near future[9]. In NEMOH, it is also a plus that there is no limitation in defining wave frequencies and angles intervals while there are some limitations in defining these parameters in AQWA. That is why, RAO of 90 wave directions and 64 frequencies are taken from NEMOH for the second part of the thesis (significant motion calculation) which AQWA cannot perform in single run. Computation cost of OrcaWave is less compared to NEMOH and AQWA, it does not have the ability to transform the calculation reference point (without manipulating the input mesh) and check the result at desired locations other than reference point.

In the second part of the thesis, JONSWAP wave spectra are created by performing sensitivity analysis of peak shape parameter γ and implementing the correction term α in order to have good agreement with onboard measured energy spectra for all sea states. Significant wave heights obtained from JONSWAP are identical with the measured ones. Significant motions calculated from JONSWAP wave spectra also give satisfying results according to the measured spectra. The methods implemented in this thesis in defining the suitable wave spectra model and estimation of significant motions provides very useful outcome for normal operating condition at working site. Consideration of more number of sea states by the utilisation of the work presented in this thesis are recommended for

*A COMPARATIVE STUDY BETWEEN DIFFRACTIONANALYSIS SOFTWARES AND
MEASURED MOTIONS*

more promising development in the future research in all working conditions.

*A COMPARATIVE STUDY BETWEEN DIFFRACTIONANALYSIS SOFTWARES AND
MEASURED MOTIONS*

Declaration of Authorship

I declare that this thesis and the work presented in it are my own and have been generated by me as the result of my own original research.

Where I have consulted the published work of others, this is always clearly attributed.

Where I have quoted from the work of others, the source is always given. With the exception of such quotations, this thesis is entirely my own work.

I have acknowledged all main sources of help.

Where the thesis is based on work done by myself jointly with others, I have made clear exactly what was done by others and what I have contributed myself.

This thesis contains no material that has been submitted previously, in whole or in part, for the award of any other academic degree or diploma.

This thesis is subjected to a Non Disclosure Agreement and I cede copyright of the thesis in favour of DEME, Ecole Centrale de Nantes and University of Liege.

Date:

Signature:

ACKNOWLEDGEMENT

I would like to thank my supervisors Florian Stempinski and Benjamin Baert for their excellent guidance and contribution of influential ideas in my thesis. I would also like to share my gratitude to my colleagues David and Elstine at the naval team for providing the helpful ideas about NEMOH and Orcawave. Moreover, I pass my thanks to my colleagues Christophe, Sijun and Thomas at the naval team who were always friendly and helpful to me during the internship period at DEME.

On the other hand, I would like to express gratitude to Professors Philippe Rigo and Lionel Gentaz who supported me throughout this master program. Then I would like to thanks to all the professors at Ecole Centrale de Nantes who taught very well the subjects of hydrodynamics for ocean engineering which helped me a lot during this thesis.

Ei Phyu Sin Mon

Antwerp (26.08.2021)

References

- [1] European Green Deal. URL: https://ec.europa.eu/info/strategy/priorities-2019-2024/european-green-deal_en.
- [2] Inc ANSYS. *Aqwa Theory Manual*. Release 15.0, 2013.
- [3] J.M.J. Journée and W.W. Massie. *Offshore Hydromechanics*. 2001.
- [4] Lionel Gentaz. *ECN Lecture:General Concepts of Hydrodynamics*. 2020.
- [5] Guillaume Ducrozet. *ECN Lecture:Water Waves and Sea State Modelling*. 2020.
- [6] Pierre Ferrant. *ECN Lecture:Wave Structure Interactions*. 2020.
- [7] O. M. Faltinsen. *Sea Loads on Ships and Offshore Structures*. 1990.
- [8] Inc ANSYS. *Aqwa Reference Manual*. Release 2020 R1, 2020.
- [9] Aurelien Babarit. *NEMOH training*. Feb. 2016.
- [10] Pierre Benreguig Moran Charlou. *ECN Seakeeping Labwork:Using the BEM Solver NEMOH*. 2020.
- [11] David Albert. “A numerical analysis of the workability of a large offshore crane vessel with respect to windsea and swell waves”. DEME offshore, 2019.
- [12] *NEMOH-Running*. URL: <https://lheea.ec-nantes.fr/valorisation/logiciels-et-brevets/nemoh-running>.
- [13] Inc Orcina. *Orcawave Help*.
- [14] U.S. Naval Academy. *EN455: Seakeeping and Maneuvering*.
- [15] DNV-GL. *DNVGL-RP-C205-Environmental conditions and environmental loads*. 2019.
- [16] *Metocean design and operating considerations (ISO 19901-1:2005)*.